Control of the NBP linear drive system

Markus Henke*, Horst Grotstollen

Institute for Power Electronics and Electrical Drives, University of Paderborn, D-33095 Paderborn, Germany

Abstract

The control of the linear motor of the NBP railway carriage is presented in this paper. The doubly fed long-stator linear motor is designed by means of modelling, according to mechatronic methods. Next steps in mechatronic design procedures are simulation, analysis and experimental validation. The presented motor propels a mechatronic railway carriage, which is also fitted with active suspension/tilt and support/guidance modules. © 2002 Elsevier Science Ltd. All rights reserved.

Keywords: Linear motors; Modelling; Drives; Railways

1. Introduction

In conventional railway systems, the functions supporting, guiding, driving and braking are realised exclusively by means of tiny surfaces where the wheels touch the rail. The main disadvantage of this force-closed drive are the high friction between wheel and rail and the decrease in force closure in case of wet and icy rails. Systems driven by a linear motor will offer the advantage of a frictionless drive of the respective vehicle. But many of these systems require a new line of their own. The environment will be extensively affected, so that will seriously endanger future realisation. By means of mechatronic methodology the research team *Neue Bahntechnik Paderborn*/NBP has designed a mechatronic, modular railway system that combines the advantages of the two concepts (Lückel, Grotstollen, Jäker, Henke, & Liu, 1999). Such a system needs clear structuring and is based on three *Mechatronic Function Modules*/MFM (Honekamp, Stolpe, Naumann, & Lückel, 1997). Drive and brake module, suspension and tilt module and support and guidance module (Fig. 1). The drive and brake module consists of a long-stator linear motor. Every MFM is based on the consistent use of information and communication techniques.

In combination with actuators and sensors, information technique enables a novel mechatronic system with special performances. The dynamics of the controlled vehicle are determined by controllers integrated in information-processing units.

The basic propulsion concept is to realise the drive function not by way of the wheels but by a linear motor integrated into the existing rail system. By using the active suspension/tilt technology, the ride comfort will be improved. In combination with an active steering, the wear of wheels and rails will be minimised. By coupling with the passive primary suspension, these three modules make up an *Autonomous Mechatronic System*/AMS that allows to build-up the fully automated shuttle, without a driver, and for the transport both of passengers and of goods. Several shuttles linked purely by information processing are combined to make up a *Crosslinked Mechatronic System*/CMS that corresponds to the highest hierarchical level.

As the mechatronic actuator the linear drive technology provides a very important part in this concept of new train system and its further details will be treated in this paper.

To analyse the behaviour of the linear motor its mathematical model is drawn up. A control structure has to be found to deal with disturbances affecting the system. After that the overall dynamical behaviour of the drive is analysed via simulation and validated by experiments. The next step in the mechatronic design procedure is the optimisation of the overall system.

*Corresponding author. Tel.: +49-5251-603-653; fax: +49-5251-603-443.
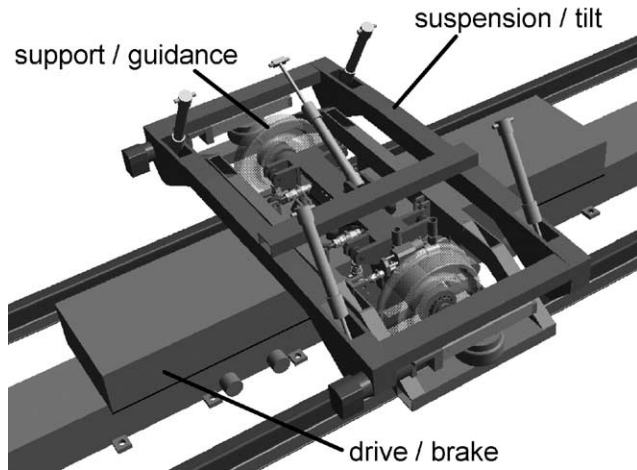
E-mail address: henke@lea.upb.de (M. Henke).

Fig. 1. Modular structure of the NBP undercarriage.

Fig. 2. Overall structure of the mechatronic drive system.

2. The system structure

The linear motor in the main consists of the primary (stator) which is installed between the rails and the secondary, being mounted on the undercarriage.

The stator is supplied with three-phase AC current, so that a magnetic travelling field is generated in the stator windings. It exerts a force on the electrically excited secondary in the carriage. Primary and secondary are interlinked magnetically by the air gap whose constant length is being ensured by the tracking of the carriage. A comfortable control of the longitudinal dynamics can be obtained because the propulsion force is directly transmitted to the secondary without any loss due to the transmission.

In order to avoid constant power supply to the entire track, it is divided into segments that are supplied with voltage by different power supply units. They index the power supply to the next position in dependence of that of the coach. As a result, the energy consumption of the drive is reduced because the track is supplied only in the respective segment where there is a coach on the stator.

The drive module comprises the power supplies, a battery module and the sensors and the information processing for vehicle and stator field control (Fig. 2).

In order to make the carriage motion flexible, a relative motion between different coaches on the same stator has to be made possible. This puts high demands on the actuators as well as on the control and information-processing units.

A synchronous long-stator linear motor is not able to produce the desired relative motion when several vehicles are operated on one stator segment; therefore the secondary in the coach will be equipped with a three-phase winding. Thus, the excitation flux can be varied relative to the position of the coach and an asynchronous operation relative to the stator field comes within
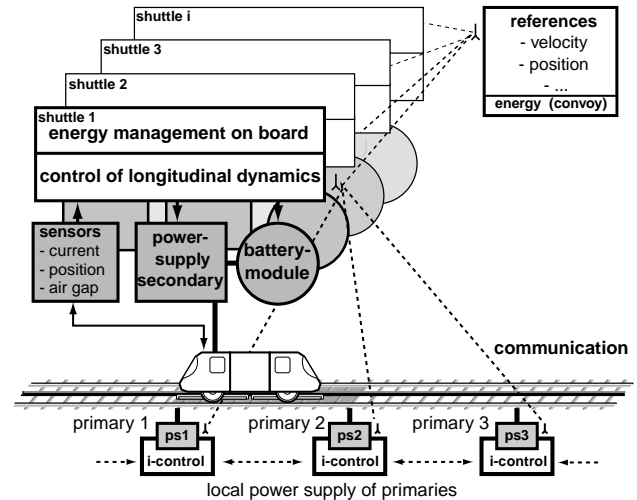
reach (Fig. 3). This operation mode does not imply the functionality of an asynchronous induction motor because the secondary currents are not inducted via the secondary flux linkage.

The actual thrust control is performed on board and the motor is doubly fed, i.e., primary and secondary can align their magnetic fluxes at any time (Henke & Grotstollen, 1999).

3. Modelling of the drive system

The primary and the secondaries share the same stator current as the stator flux linkage depends also on the magnetic flux of the secondary. The currents in the secondaries are going to be controlled according to a uniform coordinate system common to all coaches; thus the interactions between the shuttles can be traced clearly. The coordinate system employed is thus oriented according to the stator current reference vector. The reference of the stator current orientation makes up the d-axis of the coordinate system with $i_{Sq} \cong 0$.

The model of the secondary in the coach is also built-up oriented according to the stator current.

The electrical subsystem of the doubly fed linear motor relies on those of the asynchronous linear motor. Variables oriented according to the secondary are indexed R, all stator variables, S. As regards motor parameters, L_h, L_σ are the mutual and leakage inductances, R_R, R_S are the resistance of secondary and primary, ψ_R, ψ_S are the flux linkages, ω_{KS} is the angular velocity of the stator field, ω_{RS} is the angular velocity of the secondary and σ, ρ are the leakage and resistance coefficients

$$\sigma = 1 - \frac{L_h^2}{L_S L_R} \quad \text{and} \quad \rho = 1 + \frac{L_h^2 R_R}{L_R^2 R_S}.$$
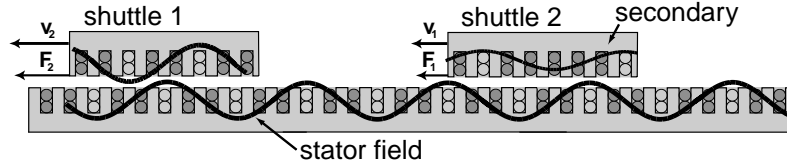
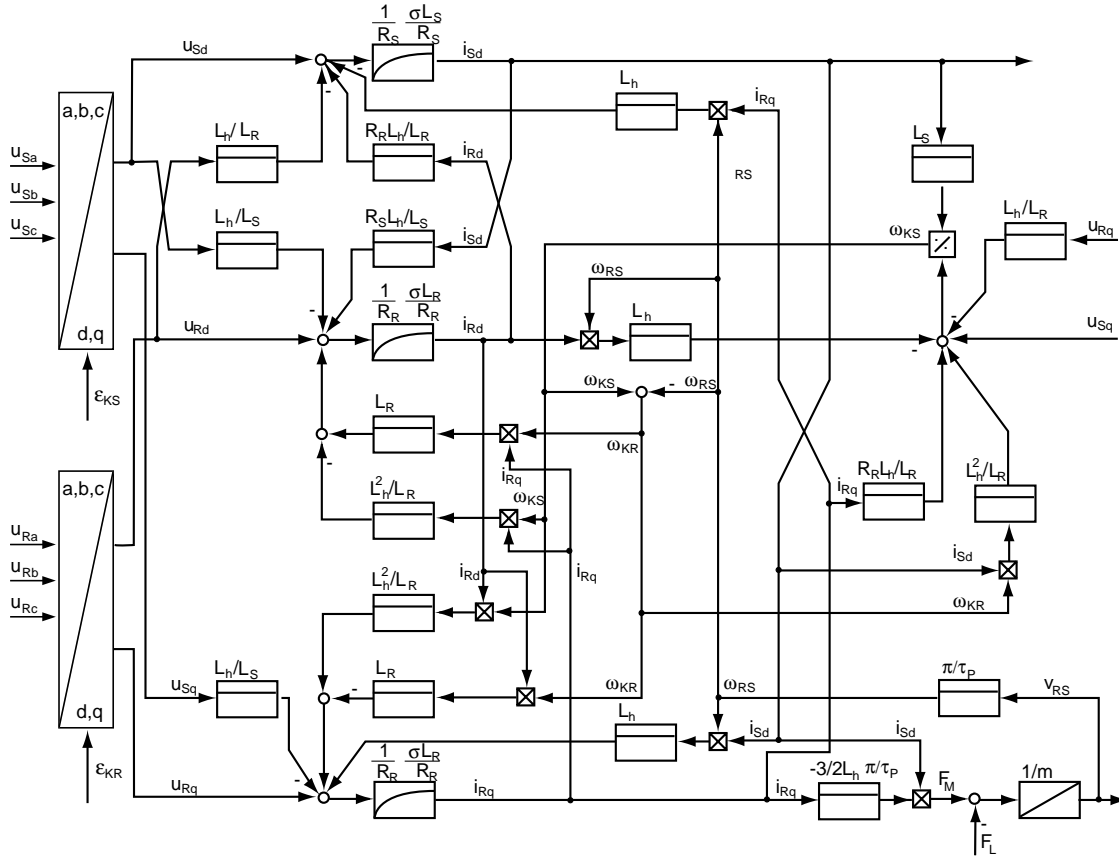Fig. 3. Thrust build-up and relative motion.

Fig. 4. Model of the doubly fed linear motor.

The values of the electrical parameters of the linear drives, related to the motor primary are: $L_h = 5.8\,\text{mH}$, $L_S = 16\,\text{mH}$, $L_R = 1\,\text{mH}$; $R_S = 0.85\,\Omega$, $R_R = 0.48\,\Omega$, $\sigma = 0.79$, $\rho = 1.19$. The equations of electrical machines can be subdivided into voltage- and force-behaviour. The complex equations relating to the voltage of the primary and secondary are displayed in (1) and (2), respectively,

$$\sigma L_S \frac{d\underline{i}_S}{dt} = \underline{u}_S - R_S \underline{i}_S - \frac{L_h}{L_R} \underline{u}_R$$
$$+ \frac{L_h R_R}{L_R} \underline{i}_R + j\omega_{RS} L_h \underline{i}_R$$
$$+ j\omega_{KR} \frac{L_h^2}{L_R} \underline{i}_S - j\omega_{KS} L_S \underline{i}_S, \tag{1}$$

$$\sigma L_R \frac{d\underline{i}_R}{dt} = \underline{u}_R - R_R \underline{i}_R - \frac{L_h}{L_R} \underline{u}_S$$
$$+ \frac{L_h R_S}{L_R} \underline{i}_S + j\omega_{RS} L_h \underline{i}_S$$
$$+ j\omega_{RS} \frac{L_h^2}{L_R} \underline{i}_R - j\omega_{KR} L_R \underline{i}_R. \tag{2}$$

The stator current oriented coordinate system is used, so that (1) and (2) have to be transformed relating to the stator current position. Transformation yields the real part of (1) as follows:

$$\sigma L_S \frac{di_{Sd}}{dt} = u_{Sd} - R_S i_{Sd} - \frac{L_h}{L_R} u_{Rd}$$
$$+ \frac{L_h R_R}{L_R} i_{Rd} - \omega_{RS} L_h i_{Rq}. \tag{3}$$

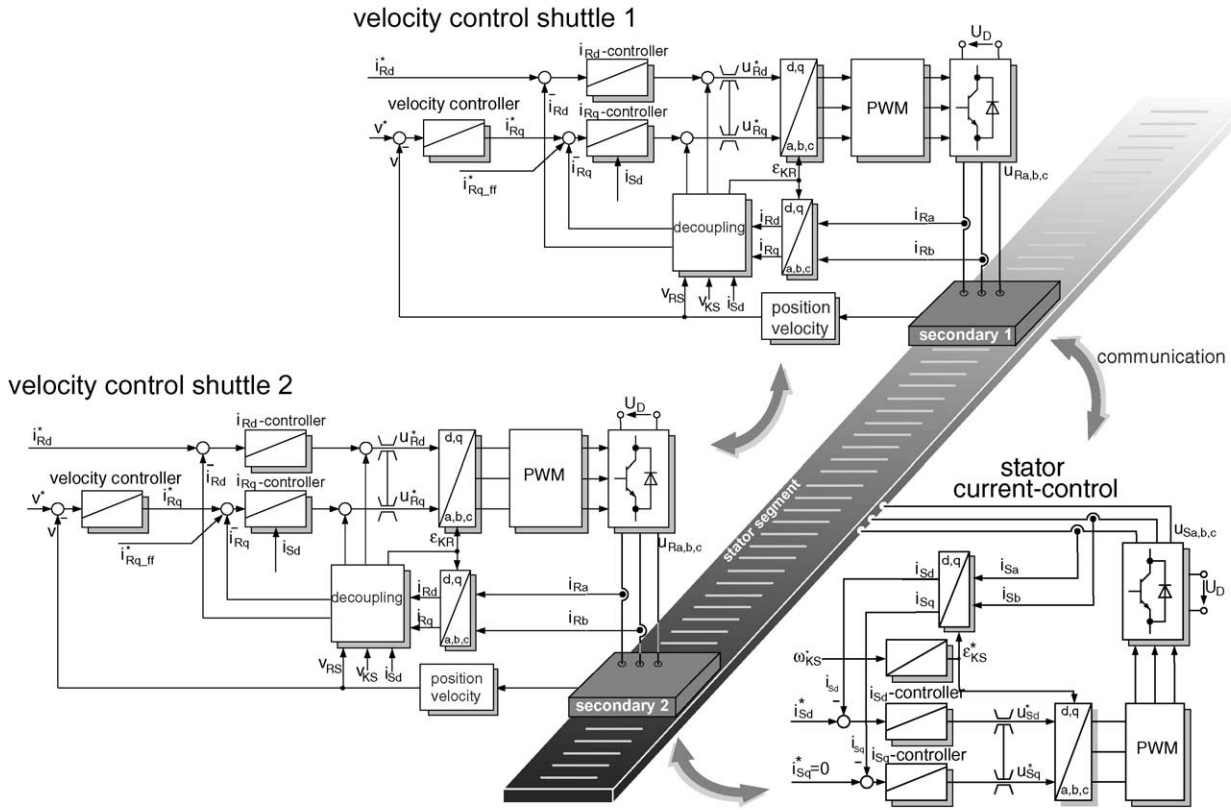Fig. 5. Control structure of two shuttles.

The imaginary part is

$$\sigma L_S \frac{\mathrm{d}i_{Sq}}{\mathrm{d}t} = u_{Sq} - R_S i_{Sq} - \frac{L_h}{L_R} u_{Rq}$$
$$+ \frac{L_h R_R}{L_R} i_{Rq} - \omega_{RS} L_h i_{Rd}$$
$$+ \omega_{KR} \frac{L_h^2}{L_R} i_{Sd} - \omega_{KS} L_S i_{Sd} = 0. \tag{4}$$

The angular frequency of the stator current results in

$$\omega_{KS} = \frac{1}{L_S i_{Sd}} \left(u_{Sq} - \frac{L_h}{L_R} u_{Rq} + \frac{L_h R_R}{L_R} i_{Rq} \right.$$
$$\left. - \omega_{RS} L_h i_{Rd} + \omega_{KR} \frac{L_h^2}{L_R} i_{Sd} \right). \tag{5}$$

The dynamics of the stator current are represented in Eqs. (3) and (4). To determine the electrical states in the secondary, the equations of the secondary voltage have to be derived; they yield the secondary current

components:

$$\sigma L_R \frac{\mathrm{d}i_{Rd}}{\mathrm{d}t} = u_{Rd} - R_R i_{Rd} - \frac{L_h}{L_S} u_{Sd}$$
$$+ \frac{L_h R_S}{L_S} i_{Sd} - \omega_{KS} \frac{L_h^2}{L_R} i_{Rq}$$
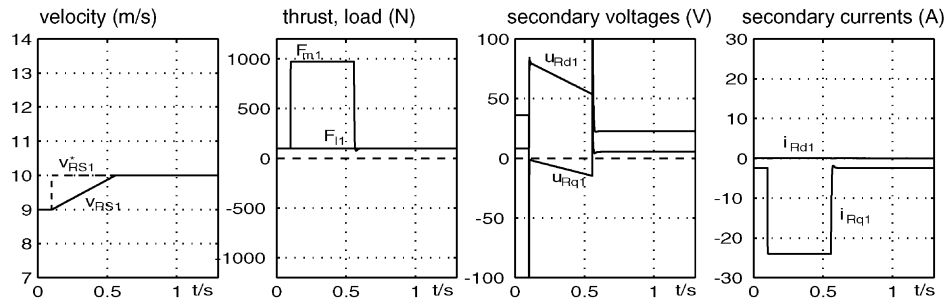$$+ \omega_{KR} L_R i_{Rq}, \tag{6}$$

$$\sigma L_R \frac{\mathrm{d}i_{Rq}}{\mathrm{d}t} = u_{Rq} - R_R i_{Rq} - \frac{L_h}{L_S} u_{Sq}$$
$$+ \omega_{RS} L_h i_{Sd} + \omega_{KS} \frac{L_h^2}{L_R} i_{Rd}$$
$$- \omega_{KR} L_R i_{Rd}. \tag{7}$$

The force equation of the motor is as follows:

$$F_m = - \frac{3\pi}{2\tau_p} L_h i_{Sd} i_{Rq}. \tag{8}$$

The thrust is proportional to the stator current i_{Sd} and to the secondary component i_{Rq}. Fig. 4 displays the block diagram of the motor. Here, five variables have to be controlled: the velocity of the coach v_{RS}, the components of the rotor current i_R, the stator current frequency ω_{KS}, and the amplitude of the stator current i_{Sd}.
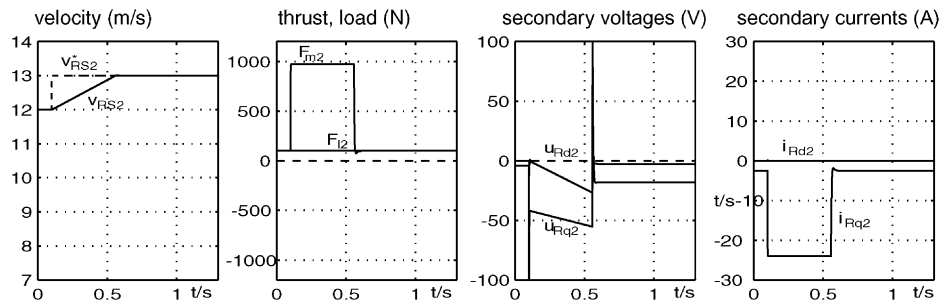
Fig. 6. Simulation results, two shuttles with different velocity on the same stator segment.
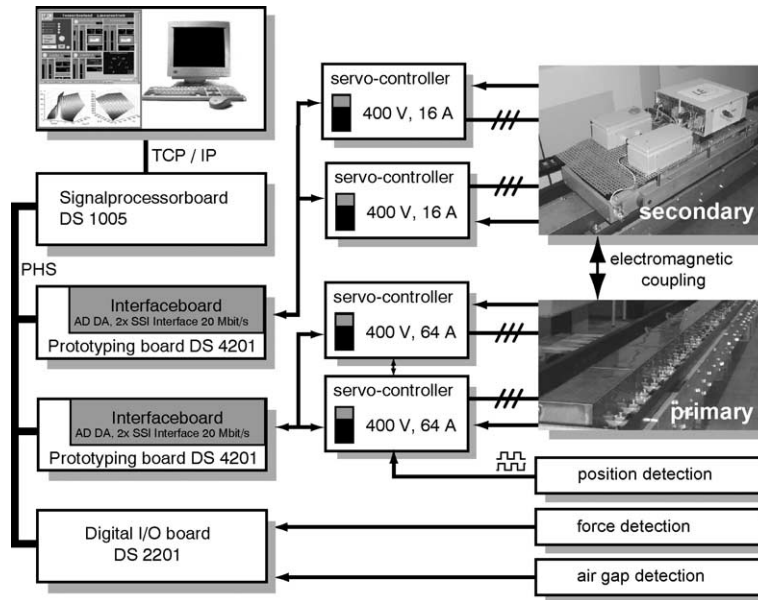

Fig. 7. Test stand for the linear drive.

4. Drive control

The system behaviour forces the decoupling of the stator field control from the control of each coach because the communication between stator control and vehicle control units cannot be realised with the bandwidth necessary for highly dynamical current control.

4.1. Control of the stator field

Contrary to conventional linear drive systems, the stator here is a unit whose current has to be controlled as to constant frequency and amplitude during operation. The reference frequency and the stator current amplitude determine the complex stator current reference vector. This vector $\underline{i}_S^*$ is transformed into the

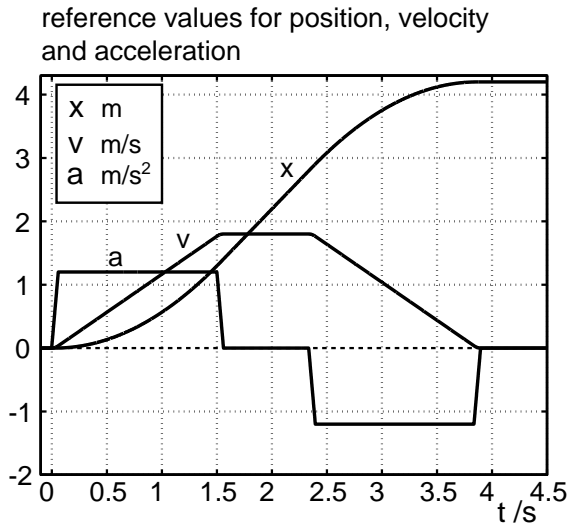reference values for position, velocity and acceleration

Fig. 8. Reference profile.

orthogonal components $i_{S\alpha}^*$ and $i_{S\beta}^*$, which represent the control variables for stator current control. So frequency control is converted to current control because the frequency itself cannot be measured directly.

The stator current frequency depends on the vehicle velocities because the slip between primary and secondary flux is used to affect the energy flow between primary and secondary (Henke, Kathöfer, & Grotstollen, 2001).

Several vehicles on the same stator segment are coupled magnetically via the stator windings. Therefore, disturbances in stator current control are the voltages induced by several shuttles operating on the same segment.

4.2. Control of the longitudinal dynamics

Every coach controls its own longitudinal dynamics via the electrical position of the secondary current and uses the stator flux common to all coaches.

The controller takes into account the switching between the stator segments. The segments the shuttle is running into, have to build-up the current just before the secondary enters the segment.

As the stator current i_{Sd} is fixed at a constant value, the only remaining actuating variable for thrust control is the q-component i_{Rq} of the secondary current, cf. Eq. (8). The stator current component i_{Sd} can be regarded as a constant excitation where the coordinate system is oriented on, so the control scheme becomes fairly similar to well-known field-oriented control. Nevertheless, both fluxes (primary and secondary) are not fixed to the mechanical position of the secondary, so that asynchronous operation becomes possible.

The actual values of the current components i_{Rd} and i_{Rq} are determined from the measured and transformed secondary currents $i_{Ra,b}$.

Fig. 5 displays, in detail, the overall structure of the coach control: A converter is generating the voltage values required by the controllers. On board, a converter supplies the on-board batteries and the three-phase windings.

For the control of the carriage, there are thus three remaining variables to be controlled: the components of the secondary current and, superordinated, the velocity v_{RS} of each carriage. All these control loops are realised with PI-controllers. The decoupling structure is used to decouple the d- and q-loops of the secondary currents.

$$u_{dec\_d} = -\omega_{KS}\frac{L_h^2}{L_R}i_{Rq} + \omega_{KR}L_Ri_{Rq}, \qquad (9)$$

$$u_{dec\_q} = \omega_{KS}\frac{L_h^2}{L_R}i_{Rd} - \omega_{KR}L_Ri_{Rd}. \qquad (10)$$

Feedforward control of velocity and secondary current yields a reduction of the position error.

The air gap between the primary and the secondary has to be assessed because a change would immediately affect thrust and braking forces. Alterations in the air gap affect the build-up of force and voltage as alterations in the gain, so the thrust controller will have to be adapted accordingly. The described control structure can be used to control several vehicles on the same stator segment. Each vehicle is fitted with local thrust and velocity control (Fig. 5).

4.3. Measurement of position and velocity

The control scheme requires the knowledge of the position of the vehicle, respectively, the position relative to the stator field. This can be obtained either by using hall elements on board for stator flux detection or by implementing an observer algorithm. The test stand used here is fitted with an incremental encoder, which measures the position directly and calculates the velocity via differentiation.

5. Simulation

A simulation model has been made for the control shown above. It includes the cascaded vehicle control and the power management of two shuttles, operating on the same stator segment. The energy flow between stator and secondary can be analysed via currents and voltages in primary and secondary.

Fig. 6 displays the simulation results. At $t = 0.1$ s, a step in the reference value of the velocity up to 10 m/s affects shuttle 1. Shuttle 2 accelerates up to 13 m/s. The stator field velocity is controlled to 12 m/s. In this
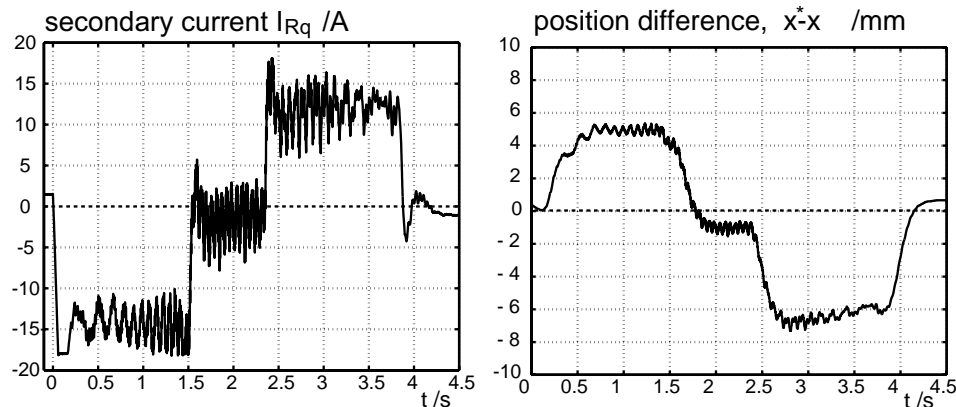
Fig. 9. Secondary current and position difference.

operation point, shuttle 1 runs subsynchronous because its velocity is lower than the stator field velocity.

Both shuttles are supplied the same secondary current i_{Rq} to run at constant speed with constant load. The secondary voltages are different and represent the difference in energy consumption. Shuttle 1 is able to reload its batteries, and shuttle 2 has to deliver energy for moving faster than the stator field. Because of different secondary velocities the secondary currents are controlled to different frequencies because the phase relation to the stator flux has to be maintained.

6. Experiments

To validate the theoretical investigations, a testbed has been built up. It is designed to reproduce the real system in 1:2.5 scale. The mass of the secondary is 120 kg, and the position range is 6.8 m.

The power supplies of primary and secondary are realised by two converters. They communicate via an interface board with the DSP-Board. The control of the stator current, and the motion control is also realised on the digital signalprocessor (Fig. 7).

The references of position, velocity and acceleration are shown in Fig. 8. They are calculated off-line and used for feedforward control.

The vehicle accelerates with a maximum acceleration of 1.2 m/s^2 up to a velocity of 1.8 m/s.

Fig. 9 shows the measured secondary current i_{Rq} and the position difference. While accelerating the current reaches its maximum. It shows oscillations which appear because of small disalignments of the position sensor which result in oscillations of velocity detections. The end of each segment is fitted with fewer windings, so that the main inductance L_h depends on the secondaries position. This yields in force disturbances which have to be compensated by the current control.

The disturbances can be stored in a characteristic scale, so that the current controller can be adapted to compensate them.

The presented test stand is fitted with a linear motor in scale 1:2.5 to real applications. Its efficiency is about 60%. For real application, the length of the primary affects the efficiency of the system, so that several vehicles should be coupled and run in convoys to increase the exploitation of the linear drive.

7. Conclusion

The presented doubly fed linear drive has been analysed by means of mechatronic methodology. The mathematical model has been set up and the equations have been analysed. A control structure with stator current orientation emerged. The longitudinal dynamics of the carriage are controlled by the linear drive, and the stator current is treated separately. Finally, experiments on the testbed close the mechatronic design procedure.

References

Henke, M., & Grotstollen, H. (1999). Regelung eines Langstator-Linearmotors für ein spurgeführtes Bahnfahrzeug. *Proceedings of the SPS/IPC drives conference 1999* Nürnberg, Germany (pp. 775–782).

Henke, M., Kathöfer, A., & Grotstollen, H. (2001). Simulation von Betriebsverhalten und Energieflüssen des NBP-Linearantriebes. *Proceedings of the ASIM 2001* Paderborn, Germany (pp. 229–234).

Honekamp, U., Stolpe, R., Naumann, R., & Lückel, J. (1997). Structuring approach for complex mechatronic systems. *Proceedings of ISATA conference on mechatronics*, Florence, Italy.

Lückel, J., Grotstollen, H., Jäker, K.-P., Henke, M., & Liu, X. (1999). Mechatronic design of a modular railway carriage. *Proceedings of the 1999 IEEE/ ASME international conference on advanced intelligent mechatronics*, Atlanta, USA (pp. 1020–1025).